Study of Water Binding to Low-Spin Fe(III) in Cytochrome P450 by Pulsed ENDOR and Four-Pulse ESEEM Spectroscopies

D. Goldfarb,*,†,‡ M. Bernardo,§ H. Thomann,*,§ P. M. H. Kroneck,⊥ and V. Ullrich⊥

Contribution from the Department of Chemical Physics, The Weizmann Institute of Science, Rehovot 76100, Israel, Exxon Research and Engineering Co., Route 22 East, Annandale, New Jersey 08801, and Faculty of Biology, University of Konstanz, Universitätstrasse 10, D-78434 Konstanz, Germany

Received April 24, 1995[⊗]

Abstract: Cytochrome P450cam (CP450cam) was studied by pulsed ENDOR and two- and four-pulse ESEEM spectroscopies. Spectra were recorded and simulated at the three principal *g*-values of the rhombic EPR spectrum. The four-pulse ESEEM experiment gave a direct measure of the anisotropic hyperfine interaction for the protons. Using the point dipole approximation this gives a Fe−H distance of 2.6 Å. The measured anisotropic hyperfine interaction reduced the number of hyperfine interaction parameters required to simulate the ENDOR line shapes. Both the four-pulse ESEEM frequencies and the ENDOR spectra at all three principal *g*-values could be satisfactorily simulated using two magnetically equivalent protons and a water orientation similar to that obtained in our previous ^{17}O ESEEM study. Thus, the pulsed ENDOR and four-pulse ESEEM results are self-consistent with the ^{17}O ESEEM data and indicate that the axial ligand is a water molecule rather than an OH^- ligand. The isotropic hyperfine value derived from the numerical simulations is in agreement with previous values derived from proton NMR relaxation studies.

Introduction

Cytochrome P450 (CP450) enzymes are ubiquitous O_2 activators consisting of a protoporphyrin IX prosthetic group as the active site.[1−4] The best characterized CP450 enzyme is the CP450 camphor from *Pseudomonas Putida*(CP450cam) for which several high-resolution crystal structures were reported.[5−9] In the substrate free CP450cam enzyme the Fe^{3+} is low spin and hexacoordinated.[5] Upon camphor binding the Fe^{3+} becomes high-spin and pentacoordinated.[6,7,10] A cysteine thiolate sulfur constitutes the proximal ligand which remains bound to the metal upon substrate binding. From X-ray diffraction studies it has been concluded that the distal ligand, which is removed upon camphor binding, is either a water molecule or a hydroxide ion, with a Fe−O distance of 2.28 Å.[5]

The possible mechanisms relating the substrate binding, the coordination number, the spin state equilibrium, and the redox potential where discussed by Poulos and Raag.[9,11] These authors also argued that OH^- is the more likely sixth axial ligand. Room temperature NMR relaxation measurements on substrate free P450cam showed a significant enhancement of the water proton relaxation[12] indicating that one or more strongly exchangeable protons, with an isotropic hyperfine constant of 2.2−3.1 MHz, are within 2.6−2.9 Å from the heme iron.[13] Electron nuclear double resonance (ENDOR) measurements also showed the existence of strongly coupled exchangeable proton(s) with hyperfine splittings that are in agreement with the NMR results.[14] The possibility that the signal is due to proton(s) bound to the cysteinyl sulfur could not, however, be ruled out.[14] In a recent communication the two broad ENDOR peaks corresponding to proton couplings of 10 and 15.2 MHz were attributed to H_2O signals in two major conformational substates of the H_2O cluster in the distal heme pocket.[15]

Recently, the binding characteristics of the distal ligand in substrate free CP450cam were measured using ^{17}O electron spin−echo envelope modulation (ESEEM) spectroscopy of the enzyme after exchange with $H_2^{17}O$.[16] From the ESEEM results the ^{17}O hyperfine and nuclear quadrupole interaction parameters were determined. Based on the magnitude and orientation of the quadrupole interaction it was concluded that at pH 7.5, the distal ligand is a water molecule rather than OH^-. The water molecule was found to be oriented with the H−O−H bisector parallel to the g_z direction which is approximately perpendicular

* Authors to whom correspondence may be addressed.

† Work by performed while on sabbatical leave at Exxon from 8/92 to 8/93.

‡ The Weizmann Institute of Science.

§ Exxon Research and Engineering Co.

⊥ University of Konstanz.

⊗ Abstract published in *Advance ACS Abstracts,* March 1, 1996.

(1) (a) Sato, R.; Omura, T. *Cytochrome P-450*; Academic Press: New York, 1979. (b) Hayaishi, O. *Molecular Mechanism of Oxygen Activation*; Academic Press: New York, 1994.

(2) White, R. E.; Coon, M. J. *Annu. Rev. Biochem.* **1980**, *49*, 315.

(3) Coon, M. J.; White, R. E. *Dioxygen Binding and Activation by Metal Centers*; Spiro, T., Ed.; John Wiley and Sons: New York, 1980; pp 73−123.

(4) Murray, R. I.; Fisher, M. T.; Debrunner, P. G.; Sligar, S. G. *Metalloproteins*, Harrison, P. M., Ed.; Verlag Chemie: Florida, Basel 1985; Vol. I, pp 157−206.

(5) Poulos, T. L.; Finzel, B. C.; Howard, A. *J. Biochemistry* **1986**, *25*, 5314.

(6) Poulos, T. L.; Finzel, B. C.; Gunsalus, I. C.; Wagner, C. W.; Karaut, J. *J. Biol. Chem.* **1985**, *260*, 16122.

(7) Poulos, T. L.; Finzel, B. C.; Howard, A. *J. Mol. Biol.* **1987**, *195*, 687.

(8) Raag, R.; Poulos, T. L. *Biochemistry* **1989**, *28*, 7586.

(9) Raag, R.; Poulos, T. L. *Biochemistry* **1989**, *28*, 917.

(10) Tsai, R.; Yu, C. A.; Gunsalus, I. C.; Peisach, J.; Blumberg, W.; Orme-Johnson, W. H.; Beinert, H. *Proc. Natl. Acad. Sci. U.S.A.* **1970**, *66*, 1157.

(11) Poulos, T. L.; Raag, R. *FASEB J.* **1992**, *6*, 674.

(12) Griffin, B. W.; Peterson, J. A. *J. Biol. Chem.* **1975**, *250*, 6445.

(13) Philson, S. B.; Debrunner, P. G.; Schmidt, P. G.; Gunsalus, I. C. *J. Biol. Chem.* **1979**, *254*, 10173.

(14) LoBrutto, R.; Scholes, C. P.; Wagner, G. C.; Gunsalus, I. C.; Debrunner, P. G. *J. Am. Chem. Soc.* **1980**, *102*, 1167.

(15) Fann, Y.-C.; Gerber, N. C.; Osmulski, P. A.; Hager, L. P.; Sligar, S. G.; Hoffman, B. M. *J. Am. Chem. Soc.* **1994**, *116*, 5989.

(16) Thomann, H.; Bernardo, M.; Goldfarb, D.; Kroneck, P. M. H.; Ullrich, V. *J. Am. Chem. Soc.* In press.

0002-7863/96/1518-2686$12.00/0

to the heme plane (within 18°).[17] Moreover, the orientation of the H−H axis with respect to the g_x direction was found to be rather restricted, 50° ± 10°. While the simulation of the experimental spectra generated one set of parameters describing the quadrupole interaction, two possible sets of hyperfine parameters were found to reproduce the experimental spectra. For the first set, the isotropic and anisotropic components, a_{iso} and $a_\perp$, were ±2.6 and ±0.3MHz respectively, while for the second, ±0.4 and ∓1.8MHz, respectively. Both sets indicate very small ^{17}O hyperfine couplings, consistent with the unpaired electron residing predominantly in the d_{yz} orbital of Fe^{3+}.[18]

The ENDOR spectrum of the protons of the water ligand is very sensitive to their hyperfine coupling and to the specific orientation of the water ligand with respect to the heme and therefore should be related to the magnetic tensors of the ^{17}O. In this paper we present combined proton pulsed ENDOR and four-pulse ESEEM results obtained from substrate free CP450cam from which we determined the hyperfine interaction of the protons of the water ligand. The results are analyzed using the constraints on the hyperfine interaction determined from the orientation of the ^{17}O quadrupole tensor. The four-pulse ESEEM experiment is a relatively new experiment and its advantage stems from the generation of highly resolved combination harmonics[19−22] which have been found to be very useful for the determination of the anisotropic hyperfine interaction.[21−27] The magnitude of the anisotropic hyperfine interaction, $a_\perp$, of the protons was determined from the four-pulse ESEEM spectrum. The value of $a_\perp$ along with the orientation of the ^{17}O quadrupole tensor were used as initial inputs for the simulations of the ENDOR spectra. The simulations then provided the isotropic hyperfine constant and the orientation of the anisotropic hyperfine interaction with respect to the **g**-matrix. The good agreement between the simulated and experimental spectra at all three principal *g*-values confirms the assignment of the axial ligand to a water molecule (for protein at pH 7.5).

Theoretical Background. The ENDOR frequencies of protons coupled to an electronic spin, $S = {}^1/_2$, are given by:

$$\omega_{\alpha,\beta} = [(\pm {}^1/_2 A - \omega_H)^2 + {}^1/_4 B^2]^{1/2} \qquad (1)$$

where ω_H is the proton Larmor frequency and

$$A = a_{iso} + a_\perp(3\cos^2\theta - 1)$$

$$B = 3a_\perp \sin\theta\cos\theta$$

θ is the angle between the external magnetic field, $\vec{H}_o$, and the principal axis of the hyperfine tensor. Using the point-dipole approximation $a_\perp$ is given by:

$$a_\perp = \frac{g\beta g_n\beta_n}{r^3\hbar} \qquad (2)$$

where r is the electron nucleus distance.

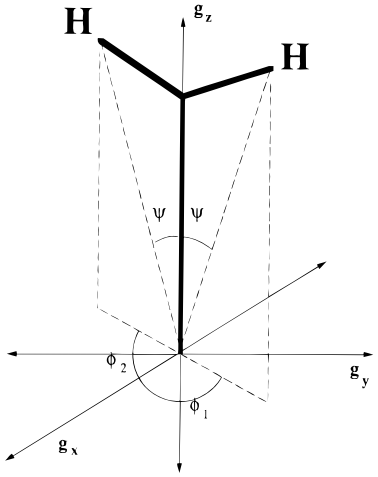

Figure 1. A schematic illustration of the water molecule orientation with respect to the principal axis system, *x*, *y*, *z*, of the **g**-matrix.

The two- and four-pulse ESEEM frequencies consist of the ENDOR frequencies $\omega_{\alpha,\beta}$ and their combinations, $\omega_\pm = \omega_\alpha \pm \omega_\beta$. For a weak coupling, $|a_\perp + 2a_{iso}| \ll 4\omega_H$, and orientational disorder (isotropic powder), the sum combination peak reaches a maximal amplitude at[26]

$$\omega_{+,max} = 2\omega_H + \frac{9a_\perp^2}{16\omega_H} = 2\omega_H + \Delta \qquad (3)$$

where Δ is the shift of $\omega_{+,max}$ from $2\omega_H$. When the EPR spectrum is dominated by a large *g*-anisotropy only a selected range of orientations of the paramagnetic center contributes to the echo due to the limited bandwidth of the microwave pulses. This range is determined by the position of the magnetic field within the EPR powder pattern. When the measurement is performed at a magnetic field corresponding to the g_z position, Δ is given explicitly by:

$$\Delta = \frac{9a_\perp^2\langle\sin^2\theta\cos^2\theta\rangle}{4\omega_H} \qquad (4)$$

where $\langle\rangle$ denotes averaging over the narrow range of selected orientations. In the above the effect of the *g*-anisotropy on the ENDOR frequencies has been neglected.

For a non-axially symmetric **g**-tensor:

$$\cos\theta = \cos\theta_o\cos\psi + \sin\theta_o\sin\psi\cos(\phi_o - \phi) \qquad (5)$$

where θ_o and ϕ_o describe the orientation of $\vec{H}_o$ with respect to the *g*-principal axes system (PAS) and ψ and ϕ relate the PAS of the axially symmetric hyperfine tensor and the **g**-tensor. These angles are defined in Figure 1.

The normalized intensity of the four-pulse echo is[20,21]

$$V(\tau,T/2) = 1 - \frac{k}{4}\left[C_o + 2C_\alpha\cos\left(\frac{\omega_\alpha}{2}(\tau+T)\right) + 2C_\beta\cos\left(\frac{\omega_\beta}{2}(\tau+T)\right) + 2C_c\left\{c^2\cos\left(\frac{\omega_+}{2}(\tau+T)\right) - s^2\cos\left(\frac{\omega_-}{2}(\tau+T)\right)\right\}\right] \qquad (6)$$

(17) Devaney, P. W. Thesis Electron spin resonance study of single crystals of cytochrome P450 from pseudomonas putida. University of Illinois, Urbana, IL, 1980.
(18) Taylor, C. P. S. *Biochem. Biophys. Acta* **1977**, *491*, 137.
(19) Gemperle, C.; Aeble, G.; Schweiger, A.; Ernst, R. R. *J. Magn. Reson.* **1990**, *85*, 241.
(20) Schweiger, A. *Modern Pulsed and Continuous-Wave Electron Spin Resonance*; Kevan, L., Bowman, M. K., Eds.; Wiley: New York, 1990; pp 43−118.
(21) Tyryshkin, A. M.; Dikanov, S. A.; Goldfarb, D. *J. Magn. Reson. A* **1993**, *105*, 271.
(22) Dikanov, S. A.; Astashkin, A. V.; Tsvetkov, Yu. D. *Chem. Phys. Lett.* **1988**, *144*, 251.
(23) Astashkin, A. V.; Dikanov, S. A.; Tsvetkov, Yu. D. *Chem. Phys. Lett.* **1988**, *144*, 258.
(24) Evelo, R. G.; Dikanov, S. A.; Hoff, A. G. *Chem. Phys. Lett.* **1989**, *157*, 25.
(25) Astashkin, A. V.; Dikanov, S. A.; Tyryshkin, M. M.; Tsvetkov, Yu. D. *Chem. Phys. Lett.* **1989**, *164*, 299.
(26) Reijerse, E. J.; Dikanov, S. A. *J. Chem. Phys.* **1992**, *95*, 836.
(27) Tyryshkin, A. M.; Dikanov, S. A.; Evelo, R. G.; Hoff, A. J. *J. Chem. Phys.* **1992**, *97*, 42.

where

$$C_o = 3 - \cos\omega_\beta\tau - \cos\omega_\alpha\tau - s^2\cos\omega_+\tau - c^2\cos\omega_-\tau$$

$$C_\alpha = c^2\cos\left(\omega_\beta\tau - \frac{\omega_\alpha\tau}{2}\right) + s^2\cos\left(\omega_\beta\tau + \frac{\omega_\alpha\tau}{2}\right) - \cos\left(\frac{\omega_\alpha\tau}{2}\right)$$

$$C_\beta = c^2\cos\left(\omega_\alpha\tau - \frac{\omega_\beta\tau}{2}\right) + s^2\cos\left(\omega_\alpha\tau + \frac{\omega_\beta\tau}{2}\right) - \cos\left(\frac{\omega_\beta\tau}{2}\right)$$

$$C_c = -2\sin\left(\frac{\omega_\alpha\tau}{2}\right)\sin\left(\frac{\omega_\beta\tau}{2}\right)$$

$$c^2 = {}^1/_2(1 + (1-k)^{1/2}) \quad s^2 = {}^1/_2(1 - (1-k)^{1/2})$$

$$k = \left(\frac{\omega_I B}{\omega_\alpha\omega_\beta}\right)^2$$

The relative intensity of the sum combination peak is given by ${}^1/_2kC_cc^2$. The intensity of the four-pulse echo in the case of two interacting protons is[21]

$$\langle V(\tau,T/2)\rangle = \langle V_1(\tau,T/2)V_2(\tau,T/2)\rangle \qquad (7)$$

where the brackets represent the orientational averaging.

Experimental Section

Sample Preparation. The substrate free CP450cam protein was purified following the procedure of Gunsalus and Wagner.[28] The material isolated contained approximately equal amounts of high- and low-spin Fe^{3+} CP450. The low-spin form was separated by passing it over a G15 Sephadex column, 0.25 mM protein in 0.3 M TRIS/HCL, pH 7.5. The sample was analyzed by continuous wave X-band EPR spectroscopy showing the typical rhombic powder pattern of low-spin CP450cam.[10]

ESEEM and Pulse ENDOR Measurements. The measurements were performed at 1.8 K using a home-built spectrometer described elsewhere.[29] The ENDOR measurements were recorded using the Davies ENDOR sequence:[30]

$$\begin{array}{ll} \text{MW} & \pi - \tau_m - \pi/2 - \tau - \pi - \tau - \text{echo} \\ \text{RF} & \pi \end{array}$$

The lengths of microwave (MW) π and $\pi/2$ pulses were 0.10 and 0.05 μs, respectively, while the radio frequency (RF) pulse width was 6.0 μs. τ was set to 0.23 μs and the repetition rate was 50 Hz. In alternating scans the phase of the echo forming pulses was varied by 180°, reversing the sign of the echo thereby eliminating baseline offsets.

The two-pulse ESEEM waveforms were recorded with the sequence $\pi/2-\tau-\pi-$echo and the same phase cycle described above was used. The pulse lengths used were 0.03 and 0.05 μs, respectively. The four-pulse ESEEM waveforms were recorded employing the sequence[19,20]

$$\pi/2-\tau-\pi/2-T/2-\pi-T/2-\pi/2-\tau-\text{echo}$$

The length of all pulses in this sequence was 0.02 μs and the amplitude of the π pulse was twice that of the $\pi/2$ pulses. This was achieved using two different pulse channels where both the phases and the amplitudes of the pulses can be varied independently. A four-step phase cycle, $+(0,0,0,0)$, $-(0,0,0,\pi)$, $+(0,0,\pi,0)$, $-(0,0,\pi,\pi)$, was employed to eliminate unwanted features in the echo envelope.[19] In both the ENDOR and the ESEEM experiments the boxar integrator was set to the center of the inverted echo. The magnetic field was measured with a Bruker Hall effect field controller calibrated against a Bruker gaussmeter. The magnetic field values used in the simulations where the values read from the field controller. Comparison with the actual field at the sample as determined from the proton Larmor frequency showed a ±20 G variation. This difference is due to the different positions of the sample and the gaussmeter. In this paper we present measured frequencies in MHz, namely, $\nu = \omega/2\pi$. The Fourier transforms of the ESEEM waveforms are shown in the absorption mode, i.e., cos FT, which was obtained after removing the background decay of the waveform and phase correcting. The initial part of the ESEEM waveform not observed due to the "dead time" of the spectrometer was not reconstructed.

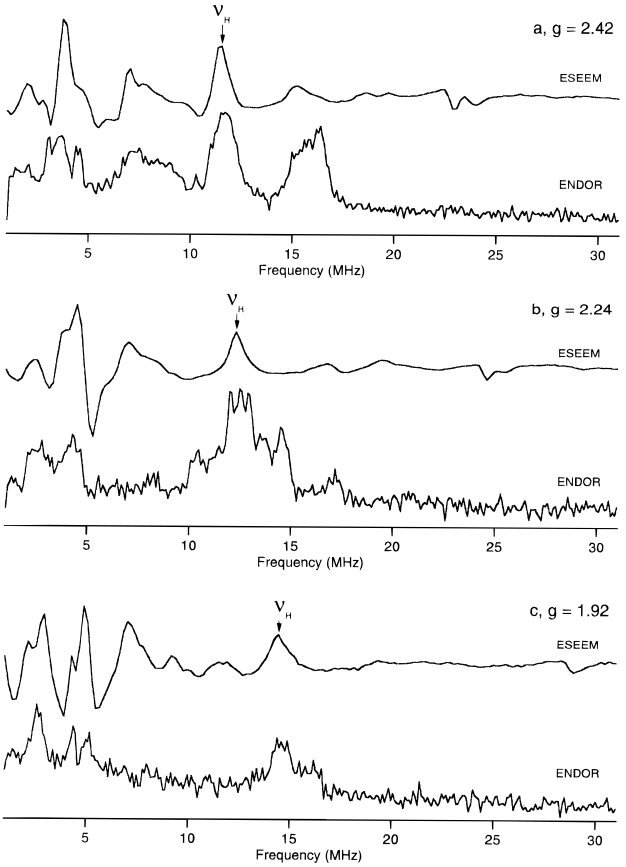

Figure 2. Two-pulse cos-FT-ESEEM and pulsed ENDOR spectra of CP450 recorded at $g = 2.42, 2.24, 1.92$. The ENDOR spectra were recorded at 2733, 2939, and 3445 G. For all measurement τ was 0.23 μs.

Results

The experiments were performed at three magnetic fields within the EPR powder pattern, corresponding to g-values close to the principal g-values, $g_x = 1.907$, $g_y = 2.26$, $g_z = 2.45$.[10] Figure 2 shows Davies ENDOR spectra, recorded at 2733, 2939, and 3445 G, corresponding to $g = 1.92$, 2.24, and 2.42, respectively. Signals below 5 MHz are assigned to heme nitrogens.[14,15] They have been previously discussed[14,15] and are not the subject of this work. The ENDOR spectrum recorded at $g = 2.42$ shows a broad structured peak at 11.6 MHz which is the proton Larmor frequency, ν_H, and a doublet at 7.5 and 16.5 MHz (9 MHz splitting) centered about ν_H. Each of the doublet components exhibits a line shape attributed either to a powder pattern for one type of proton or for two protons with different hyperfine couplings. A similar doublet, although without such a clear line shape, was observed in the X-band CW ENDOR spectrum of low-spin CP450.[14] Moreover, the protons responsible for this signals were found to be exchangeable.[14] Based on these previous results and on the analysis of the ^{17}O ESEEM,[16] we assign the proton doublet obtained at $g = 2.42$ to the protons of the axial water ligand. Below we show

(28) Gunsalus, I. C.; Wagner, C. W. *Meth. Enzymol.* **1978**, *52*, 166.
(29) Thomann, H.; Bernardo, M. *Spectrosc. Int. J.* **1990**, *8*, 119.
(30) Davies, E. R. *Phys. Lett. A* **1974**, *47A*, 1.

that the line shape originates from the powder pattern characteristics arising from the orientation selectivity due to g anisotropy and to the fact that the principal axes of the g- and hyperfine tensors are not exactly co-linear ($\psi \neq 0$, see Figure 1).

Four doublets are resolved in the ENDOR spectrum recorded at $g = 2.24$. These are centered about ν_H and have splittings of 9, 4.2, 2.4, and 0.95 MHz. The 9-MHz splitting is close to that observed in the $g = 2.42$ spectrum and is therefore also assigned to the protons of the water ligand. The inner doublets are attributed to protons on the heme and/or on the cysteine ligand. Proton hyperfine splittings observed in the low-spin CN complex of metmyoglobin and protohemin[31] and in low-spin bis(imidazole) ligated ferri heme complexes[32] do not exceed 4 MHz. It is also plausible that one (or more) of the inner doublets belongs to the powder pattern of the water protons. This possibility, as shown below, can be verified by numerical simulations of the ENDOR line shapes. Although the S/N of the spectrum recorded at $g = 1.92$ is relatively poor a broad peak at ν_H and a broad unresolved doublet centered about ν_H with a splitting of about ~3 MHz are clear. Comparison of this spectrum and that observed at $g = 2.42$ indicates that the hyperfine interaction of the water protons is highly anisotropic. The reason for the rather low S/N, compared to the spectra recorded at $g = 2.42$ and 2.24, is not clear because all spectra were obtained under similar conditions. It may partly (but not completely) originate from the limited number of orientations excited in the EPR powder pattern spectrum at $g = 1.92$.

The two-pulse ESEEM spectrum of substrate free CP450 was also measured since it provides complementary information to that obtained by ENDOR spectroscopy. ESEEM is particularly sensitive to the anisotropic part of the hyperfine interaction since the latter is essential for the observation of electron spin−echo envelope modulation. Therefore, by comparing the ESEEM and ENDOR spectra it is possible to gain insight into the relative contributions of the isotropic and anisotropic hyperfine interactions. Figure 2 presents a comparison of the pulsed ENDOR spectra and the two-pulse Fourier transform (FT) ESEEM spectra recorded at the same field values. The line shapes expected from ENDOR and ESEEM are different due to the orientation dependence of the modulation amplitudes,[33] the effect of spectrometer deadtime,[34] and the appearance of combination harmonics in the ESEEM spectra. These differences are obvious in all spectra shown in Figure 2. The doublet with the 9-MHz splitting is also clear in the ESEEM spectrum recorded at $g = 2.42$, although the line shape is different from that of the ENDOR spectrum. Moreover, combination peaks at $\nu_H \pm \nu(^{14}N)$, where $\nu(^{14}N)$ corresponds to the ^{14}N peak at 3.7 MHz, are superimposed on the 9-MHz doublet. Other line shape features on the low-frequency side of the doublet may also arise from combination harmonics of the nitrogen peaks. The line shape structure arising from these combination harmonics is very prominent in the low-frequency region (7 to 10 MHz) of the doublet in the spectra recorded at $g = 2.24$ and 1.92.

The lower resolution of the ESEEM spectrum as compared to the ENDOR spectrum in the region of ν_H is most evident in the spectrum recorded at $g = 2.24$ where the ν_H signal dominates the spectrum and the other doublets and line shape structure

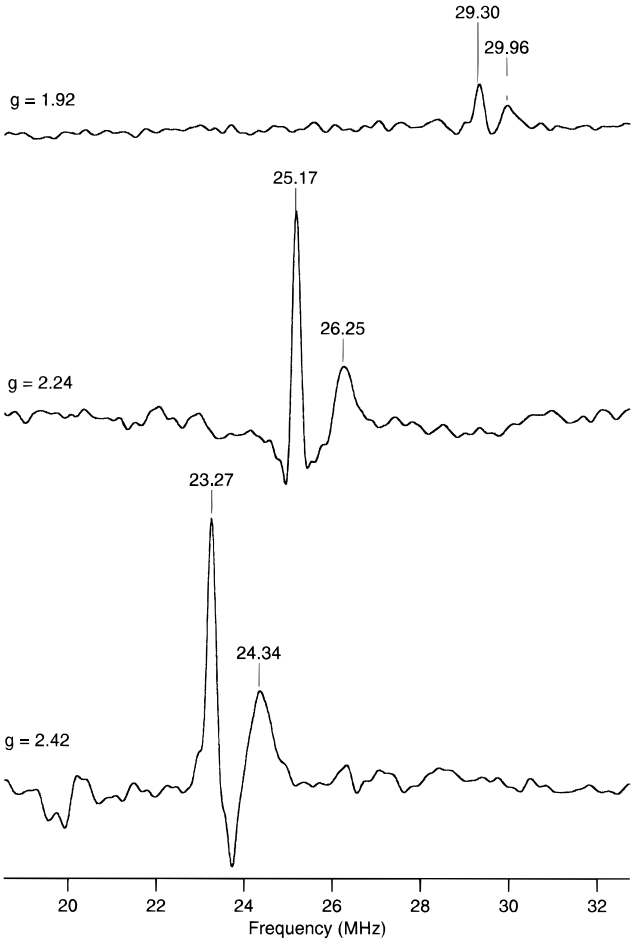

Figure 3. Four-pulse cos-FT-ESEEM spectra of CP450cam recorded at 2722, 2957, and 3449 G. The τ values were 0.24, 0.28, and 0.30 μs, respectively. Only the region of the proton sum combination harmonics is shown.

observed in the ENDOR spectrum are absent. However, one advantage of the ESEEM spectrum is the appearance of combination harmonics in the $2\nu_H$ region from which the anisotropic hyperfine interaction can be directly determined.[21−27] These combination harmonics are observed as negative peaks in the spectra recorded at all three g-values. In the ESEEM spectra recorded at $g = 2.42$ and 2.24 two peaks are resolved in the $2\nu_H$ region of the spectra. One peak corresponds to the sum combination harmonic of the matrix protons and the high-frequency shoulder corresponds to more strongly coupled protons. In contrast, the proton combination peaks in the spectrum recorded at $g = 1.92$ are not resolved.

Significantly better resolved proton combination harmonics can be obtained by the four-pulse ESEEM experiment. Figure 3 shows the four-pulse FT-ESEEM spectra in the region of $2\nu_H$, recorded at the same three g-values corresponding to the ENDOR and two-pulse ESEEM spectra shown in Figure 2. The resolution is significantly improved, particularly in the $g = 1.92$ spectrum where two ^1H combination peaks are clearly detected. Table 1 summarizes the four-pulse ESEEM results and lists the values of $a_\perp$ calculated from the shift of the sum harmonic peak using eq 3 and the r value determined from $a_\perp$ using eq 2. The g-values used in the calculations are the effective g at the field at which the measurement was performed.

The four-pulse ESEEM results give a distribution of $a_\perp$ values in the range of 4.2−4.9 MHz (Table 1). These were calculated assuming an isotropic powder distribution which is not valid for the measurements performed at $g = 2.42$ and 1.92. However, near g_y a rather broad range of orientations is selected.

(31) Mulks, C. F.; Scholes, C. P.; Dickinson, L. C.; Lapidot, A. *J. Am. Chem. Soc*. **1979**, *101*, 1645.
(32) Scholes, C. P.; Felkowski, K. M.; Chen, S.; Bank, J. *J. Am. Chem. Soc*. **1986**, *108*, 1660.
(33) Astashkin, A. V.; Dikanov, S. A.; Tsvetkov, Yu. D. *Chem. Phys. Lett*. **1985**, *122*, 259.
(34) Astashkin, A. V.; Dikanov, S. A.; Tsvetkov, Yu. D. *Chem. Phys. Lett*. **1985**, *136*, 204.

Table 1. The Shifts, Δ, $a_\perp$, and r Calculated from the Four-Pulse Data

H_o (G)	g_{eff}	$2\nu_H$ (MHz)	$2\nu_H + \Delta$ (MHz)	Δ (MHz)	$a_\perp$ (MHz)	r (Å)
2722	2.42	23.26	24.34	1.074	4.71	2.72
2957	2.24	25.17	26.26	1.075	4.90	2.62
3449	1.92	29.30	29.96	0.66	4.15	2.63

Therefore the value of $a_\perp$ calculated from the $g = 2.24$ spectrum should be more accurate. This yields $r = 2.62$ Å and $a_\perp = 4.34$ MHz for $g = 2$. The experimental uncertainty in Δ is approximately 0.1 MHz. The uncertainty in $a_\perp$ is proportionately smaller since it depends on the square root of Δ. The larger uncertainties in the $a_\perp$ values listed are not determined from experimental limits but rather from the approximations inherent in using eq 3 rather than eq 4. We estimate the uncertainty in $a_\perp$ to be ± 0.15 MHz.

Only protons with a relatively large anisotropic hyperfine interaction contribute to the shifted proton sum combination peak. Since the heme protons are known to have relatively small hyperfine couplings[35] we attribute the ^{1}H shifted peak to the water ligand protons, namely, those responsible for the 9-MHz splitting in the $g = 2.42$ ENDOR spectrum. Further quantitative analysis of the ENDOR and ESEEM spectra was obtained by numerical simulations of the orientation selective spectra. These were performed in order to substantiate the above assignment, to account for the ENDOR line shapes, to obtain a_{iso}, and to determine the orientation of the Fe−H axis with respect to the PAS of the **g**-tensor.

ENDOR Simulations. The orientations selected at each magnetic field, H_o, were determined by simulating the EPR spectrum and searching for all the **g**-tensor orientations giving rise to an absorption at $H_o \pm 0.5\delta$, where δ is the EPR inhomogeneous line width. The bandwidth of the microwave pulse was not taken into account as it is narrower than the inhomogeneous line width. The final spectrum was obtained by summing over all the selected orientations using the following weighing function:

$$G(\theta_o,\phi_o,H) = e\left\{\frac{-1}{2}\left[\frac{H_o - H}{\sigma}\right]^2\right\} \sin\theta_o \, d\theta_o \, d\phi_o \qquad (8)$$

and $\delta = \sigma/2.345$. Detailed discussions of the ENDOR line shapes expected from angle selected ENDOR spectroscopy have been reported by Hurst *et al.*[36] and Hoffman *et al.*[37]

The proton ENDOR simulations were guided by the results previously obtained from the ^{17}O ESEEM analysis.[16] Therefore, only the case of two magnetically equivalent protons with the H−O−H bisector parallel to the g_z direction was considered.[16] Referring to Figure 1, $\psi_1 = \psi_2 = \psi$ and $\phi_2 = \phi_1 + 180°$ [16] and the two protons thus have the same values of a_{iso} and $a_\perp$. At each magnetic field, $a_\perp$ was taken as $4.34 g_{eff}/2.0$ MHz. The ENDOR frequencies were calculated using eqs 1 and 6 and the weighing factor given in eq 8. The hyperfine enhancement factor was not taken into account in the simulations. This is a reasonable approximation since in the case of pulsed ENDOR experiments, once the nutation angle for the NMR transition is greater than π the ENDOR amplitudes become relatively insensitive to the hyperfine enhancement.[38,39]

For each simulated ENDOR spectrum the line shape of the corresponding $\omega_\alpha + \omega_\beta$ peak in the four-pulse ESEEM spectrum was calculated and the position of its maximum amplitude was determined. There, an additional weighing factor given by $^1/_2 k C_c c^2$ was used (see eq 6). The position of the maximum intensity of this peak is listed near each simulated ENDOR spectrum. These should be compared with the experimental positions given in Figure 3. In principle, when two interacting nuclei are present eq 7 should be used to obtain the four-pulse echo intensity. However, when k is small (in our case it is $\approx$0.12) the contributions to the sum harmonic peaks arise mostly from terms with the C_c coefficient (see eq 6) of each nucleus. The intensity of other combination peaks is proportional to $k_1 k_2$, where the indices 1 and 2 correspond to the different nuclei. This product is negligible compared to the individual k's. Thus, the line shape of the sum harmonic peak can be calculated by taking a superposition of the combination peaks of each nucleus as in the ENDOR simulations.

The 9-MHz splitting appearing in both the g_z and g_y spectra indicates that $a_{iso} + 2a_\perp \approx 9$ MHz and that ψ is small. The effects of ψ on the hyperfine splitting and on the line shape are shown in Figure 4, where simulated ENDOR spectra calculated for the three different fields, 2733, 2939, and 3445 G, are shown. The variation of ψ corresponds either to a change in the HOH angle or to a tilt of the HOH plane away from the g_z direction. The latter was found to be approximately along the heme normal[4,17] (see Figure 1). Obviously, the variation considered for ψ has a larger acceptable range compared to possible variations in the bond HOH angle.

Generally, increasing ψ reduces the splitting of the doublet of the $g = 2.42$ spectrum. It also affects the width of each ENDOR line component. The greatest line width is obtained for ψ values in the range of 30−60° since the Fe−H direction assumes more orientations with respect to $\vec{H}_o$, increasing the orientational "disorder". At very low values of ψ the line shape of the $g = 2.42$ ENDOR spectrum is not well reproduced and the splitting between the outer spectral features in the $g = 2.24$ spectrum is too small. Further increase in ψ increases the splittings of the outer spectral features in the $g = 2.24$ spectrum which is accompanied by an increase in the width of the doublet components in the $g = 2.42$. The spectra calculated with $\psi = 30°$ show a reasonable agreement with the experimental results. In particular the powder pattern of the doublet in the $g = 2.42$ spectrum and the outer spectral features in the $g = 2.24$ spectrum are reproduced. These are the most reliable features for comparison between the experimental and calculated spectra as they are unambiguously assigned to the exchangeable protons.[14] Note that the simulated $g = 2.42$ spectrum also reproduces the asymmetry of the doublet both in amplitude and in width. This asymmetry originates from the second-order hyperfine interaction represented by the B term in eq 1.

As mentioned earlier, the other signals with smaller coupling values may be due to heme protons and/or to parts of the powder pattern of the exchangeable protons. This complicates the comparison between experimental and calculated spectra at $g = 2.24$ and 1.92. Based on these simulations the peak centered at ν_H in the $g = 1.92$ spectrum is assigned to the water protons whereas the $\approx$3 MHz doublet is attributed to the heme protons. This assignment is further supported by the small anisotropy of the heme protons.[31,32] Further increase of ψ yields a $g = 2.42$ spectrum which differs significantly from the experimental

(35) Scholes, C. P.; Lapidot, A.; Mascarenhas, R.; Inubushi, T.; Issacson, R. A.; Feher, G. *J. Am. Chem. Soc.* **1982**, *104*, 2724.
(36) Hurst, G. C.; Henderson, T. A.; Kreilick, R. W. *J. Am. Chem. Soc.* **1985**, *107*, 7294.
(37) Hoffman, B. M.; Venters, R. A.; Martinsen, J. *J. Magn. Reson.* **1985**, *62*, 537.
(38) Thomann, H.; Bernardo, M. *Biological Magnetic Resonance*; Berliner, L. J., Reuben, J., Eds.; Plenum Press: New York, 1993; Vol. 13, p 275.
(39) Tan, X.; Bernardo, M.; Thomann, H.; Scholes, C. P. *J. Chem. Phys.* **1995**, *102*, 2675.

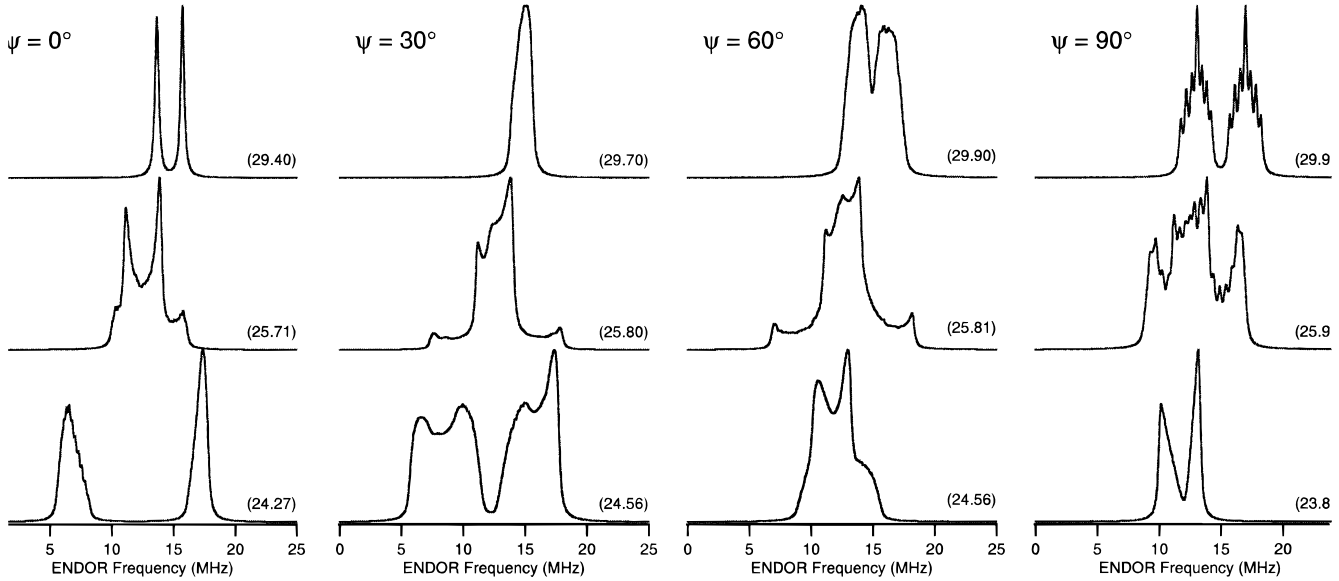

Figure 4. Simulated ENDOR spectra showing the effect of ψ for $H_o = 2733$, 2939, and 3445 G calculated with the following parameters: $a_{iso} = 2.0$ MHz $a_\perp = 4.34$ MHz, $\phi_1 = 45°$, $\phi_2 = 225°$, $\delta = 50$ G, and $\psi = 0$, 30°, 60°, and 90°. The number at the left-hand side of each spectrum gives the position of the corresponding four-pulse ESEEM sum combination peak.

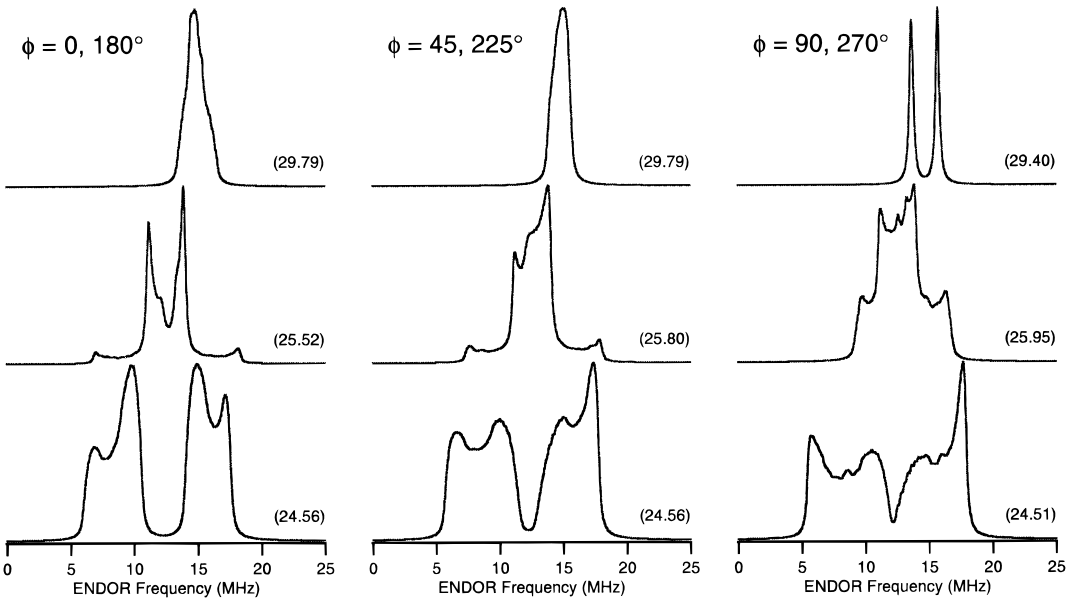

Figure 5. Simulated ENDOR spectra showing the effect of ϕ_1/ϕ_2. All parameters are as in Figure 4 but $\psi = 30°$ and $\phi_1/\phi_2 = 0°/180°$, 45°/225°, and 90°/270°. The number at the left-hand side of each spectrum gives the position of the corresponding four-pulse ESEEM sum combination peak.

spectrum. The numerical "noise" in the $g = 2.24$ and 1.92 spectra for $\psi = 90°$ is due to insufficiently small integration steps.

Having established that ψ is approximately 30° we next investigated the effect of ϕ_1 on the ENDOR line shapes as shown in Figure 5. The variation of ϕ_1 corresponds to a rotation of the Fe−H axis about the z axis (see Figure 1). This defines the orientation of the water molecule with respect to the x and y axes, which were found to be nearly within the heme plane.[4,17] In the $g = 2.42$ spectrum ϕ_1 affects both the width and the relative intensity of the maxima in the powder pattern for each of the doublet components. Increasing ϕ_1 reduces the amplitude of the inner edges and broadens each component. It also reduces the splitting of the outer edges in the $g = 2.24$ spectrum and increases their amplitudes. From this series of simulations it can be concluded that ϕ_1 is close to 45° and ϕ_2 close to 225°. Moreover, they suggest that the 3 MHz doublet in the $g = 1.92$ spectrum and that of the 4 MHz in the $g = 2.24$ spectrum are due to heme protons. This is in agreement with previous CW-ENDOR data on similar systems.[31,32,35]

The line shape of the ENDOR spectrum strongly depends on the orientations selected. These orientations cannot be determined very precisely. This is well illustrated in Figure 6 where the effect of a ±20 G shift for each of the fields corresponding to $g = 2.42$, 2.24, and 1.92 is shown. The parameters used for the simulations are those that gave satisfactory agreement with the experimental spectra (see figure caption). For this set of parameters, the $g = 2.42$ spectrum shows the highest sensitivity to variations in H_o. A better agreement with the experimental spectra is obtained with 2713 G rather than with the experimental value, 2733 G. An uncertainty of ±20 G can originate from an error in determining the magnetic field at the sample or to a small error in the principal g values used to determine the selected orientation. Changes of up to 0.2 MHz in the position of the maximum of the proton sum harmonic in the four-pulse ESEEM spectrum

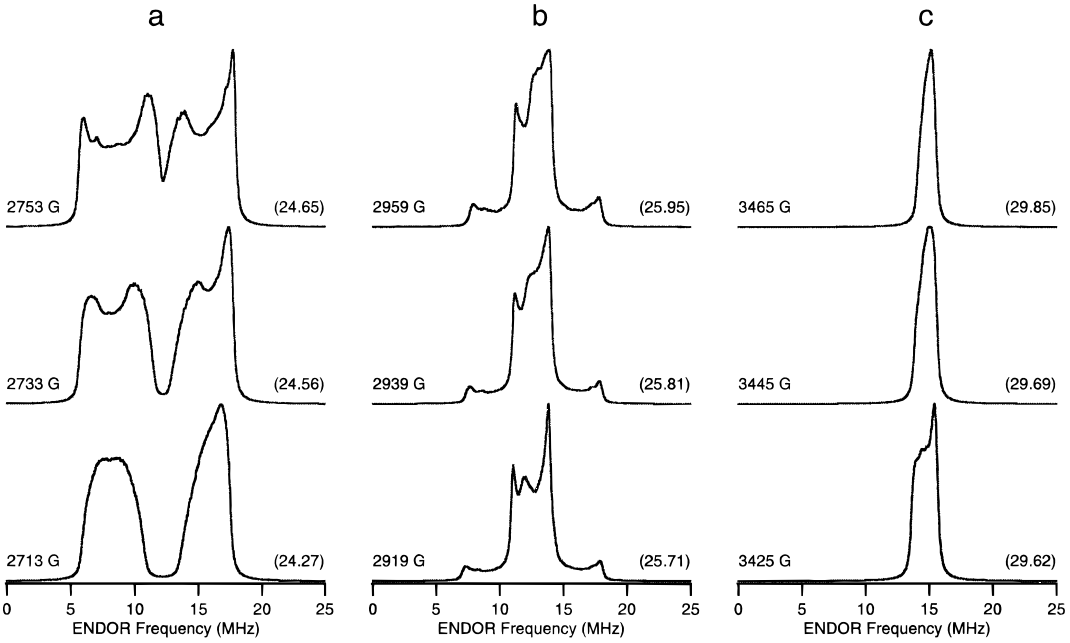

Figure 6. Simulated ENDOR spectra showing the effect of a ±20 G shift in the magnetic field on spectra recorded at $\sim g_z$, $\sim g_y$ and $\sim g_x$. The number at the left-hand side of each spectrum gives the position of the corresponding four-pulse ESEEM sum combination peak. The parameters used in the simulation are $a_{iso} = 2$ MHz, $a_\perp = 4.34$ MHz, $\psi = 30°$, $\phi_1/\phi_2 = 45°/225°$, and $\delta = 50$ G.

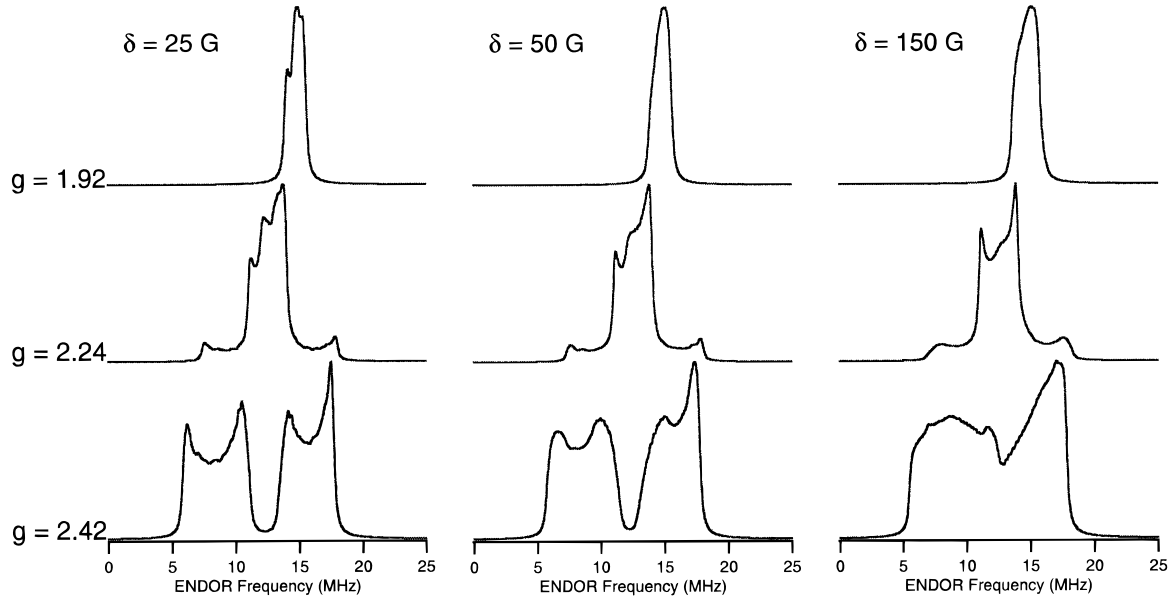

Figure 7. Simulated ENDOR spectra showing the effect of the width of the range of the selected orientation in the fields 2733, 2939, and 3445 G. The parameters used are the same as in Figure 5 and $\delta = 25$, 50, and 150 G. The numbers at the right-hand side represent the corresponding position of the four-pulse combination peaks.

can be induced by such shifts in the field. The calculated frequencies of the sum harmonic ^{1}H peaks are listed near each spectrum in Figure 6.

The inhomogeneous EPR line width also determines the range of the orientations selected. The ENDOR spectra shown in Figure 7 were calculated with the same parameters as above but with three values of the line width $\delta = 25$, 50, and 150 G. The difference between the spectra calculated for $\delta = 25$ and 50 G were found to be minor and are manifested mainly in the broadening of sharp features. Again, the spectrum recorded at $g = 2.42$ ($\approx g_z$) was found to be most sensitive to the line width selected. For $\delta = 150$ G the doublet structure disappears and a broad powder pattern is observed. The calculated position of the four-pulse sum harmonic peak was found to have a negligible dependence on the EPR inhomogeneous line width. This is in contrast to the effect of a shift in the magnetic field (or in the principal g values). This is expected as the latter causes a shift in the range of the orientations selected whereas the former only increases the range without changing its center orientation.

The signs of the $a_\perp$ and a_{iso} were taken as positive in the simulations. Reversing the sign of a_{iso} generated spectra that did not agree with the experimental results thus implying that a_{iso} and $a_\perp$ have the same sign. Taking $a_{iso} = 2$ MHz, $a_\perp = 4.34$ MHz, $\psi = 30°$, $\phi_1 = 45°$, $\phi_2 = 180°$, $\delta = 50$ G, and magnetic fields of 2722, 2957, 3449 G, which are the fields at which the four-pulse ESEEM experiments were performed, we obtained shifted sum combination harmonic peaks at 24.56, 25.91, and 29.75 MHz, respectively. This is to be compared to the experimental values of 24.32, 26.24, and 29.95 MHz. We attribute the discrepancy of ~0.2 Mhz between the calculated and experimental values to experimental error in the

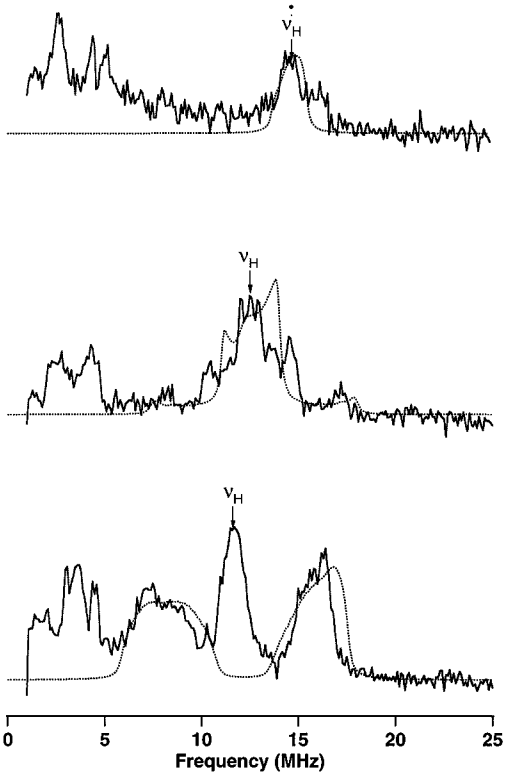

Figure 8. Comparison of the experimental ENDOR spectra in the region of ν_H (see Figure 2) and simulated spectra obtained with parameters within the best fit range, $a_{iso} = 2$ MHz, $a_\perp = 4.34$ MHz, $\psi = 30°$, $\phi_1/\phi_2 = 45°/225°$, and $\delta = 50$ G. Top: $H_o = 3465$ G. Center: $H_o = 2939$ G. Bottom: $H_o = 2713$ G.

determination of the peak positions and to the uncertainty in the determination of the selected orientations. Based on the above simulations, the following parameters were determined to give the best fit between the simulated and experimental spectra: $a_{iso} = 1.5-2.0$ MHz, $a_\perp = 4.2-4.5$ MHz, $\psi = 25-35°$, $\phi_1 = 40-50°$, $\phi_2 = 220-230°$ for the water ligand protons. A direct comparison between the experimental and simulated spectra obtained with these parameters is shown in Figure 8.

Discussion

Using the constraints on the orientation of the water ligand as determined from our previous ^{17}O ESEEM study,[16] we are able to simulate the ^{1}H pulsed-ENDOR spectra and the frequency of the ^{1}H combination harmonic in the four-pulse ESEEM spectra. This provides further supporting evidence that the sixth axial ligand in low-spin CP450cam is a water molecule rather than a hydroxide. The present results are also consistent with an earlier conclusion derived from an ^{17}O ESEEM study[16] that the water molecule exists in only one conformation. In contrast, in a recent CW Q-band ENDOR study the proton signals were assigned to two different conformational subsets of the water in the distal heme pocket.[15]

The orientation of the H−H axis with respect to the g_x orientation was determined to be 40−50°. This is in good agreement with the ^{17}O ESEEM[16] data where it was found to be distributed in the range $50 \pm 10°$. The value obtained for a_{iso} (1.5−2 MHz) also agrees with the value of 2.2−3.1 MHz estimated from proton relaxation studies.[12,13]

Assuming that $a_\perp$ can be described by the point-dipole approximation we obtain a distance of 2.62 Å between the Fe and the water protons. This value is comparable to distances between protons of water ligands and metal ions in other complexes determined by four-pulse ESEEM or ENDOR methods.[20,40,41] Taking the g_z direction along the normal to the heme plane, parallel to the Fe−O axis, we obtained for a H−O−H angle of 104° and a O−H bond length of 1 Å, an Fe−O distance of 1.87 Å and $\psi = 17.5°$. Increasing the HOH angle to 110° will give a F−O distance of 1.92 Å and $\psi = 18.2°$.

From the ^{17}O ESEEM data[16] we concluded that $|a_\perp| = 1.8$ MHz. Using the point dipole approximation, we obtain $r = 1.87$ Å which is in agreement with the value obtained from the proton dipolar coupling. The crystal structure[5] shows that there is an oxygen above the heme plane at a distance 2.28 Å from the Fe. This is somewhat larger than the value we estimated from $a_\perp$. The discrepancy of 0.3 Å could arise in part from the effect of the g-anisotropy on the ENDOR frequencies which was not taken into account in the simulations. In our calculations its affect was accounted for only by taking the effective g in eq 2, but the explicit expression, as for instance obtained for an axial **g**-tensor by Rowan et al.,[42] was not considered. Another reason for the discrepancy could be the different temperatures at which the X-ray and ESEEM/ENDOR measurements were performed. However, it is more likely that the discrepency arises from the inadequacy of the point-dipole approximation for describing the anisotropic hyperfine interaction. The presence of a pseudo-dipolar hyperfine interaction increases the value of $a_\perp$ resulting in a shorter calculated distance. This effect is commonly encountered when determining distances from the anisotropic hyperfine interaction.

Our simulations gave a somewhat larger value for ψ (25−35°) than would be expected from the distance calculated based on the point dipole approximation and assuming that g_z is along the Fe−O direction. An increase in ψ can be obtained by incresing the Fe−H distance and/or by introducing a tilt of the HOH plane with respect to the Fe−O axis. However, such a tilt, when confined to the direction that keeps the two protons magnetically equivalent (HOH bisector parallel to g_z), will introduce a very small change in ψ. For instance, a maximum tilt of 90°, for a Fe−H distance of 2.6 Å and a O−H bond length of 1 Å, yields $\psi = 22.5°$. We find, however, the discrepancy in ψ of 7−18° to be relatively small and acceptable considering that it was derived from a frozen solution sample and not from single crystal measurements.

Conclusions

Using four-pulse ESEEM and orientation selective pulsed ENDOR techniques the hyperfine interaction of the protons of the distal axial ligand in substrate free CP450cam was determined. The four-pulse ESEEM experiment gave a direct measure of the anisotropic hyperfine interaction for the protons on the water ligand from which a Fe−H distance of 2.6 Å was obtained. This reduced the number of the hyperfine interaction parameters determined from the ENDOR line shape simulations. Further reduction in the number of parameters was achieved using the constraints imposed on the water orientation from previous ^{17}O ESEEM data. The pulsed ENDOR and four-pulse ESEEM results are self consistent with our previous ^{17}O ESEEM data and indicate that at a pH of 7.5 the axial ligand is a water molecule.

JA951307E

(40) Lee, H.-I.; McCracken, J. *J. Phys. Chem.* **1994**, *98*, 12861.
(41) Atherton, N. M.; Horsewill, A. J. *J. Mol. Phys.* **1979**, *32*, 1349.
(42) Rowan, L. G.; Hahn, E. L.; Mims, W. B. *Phys. Rev. A* **1965**, *137*, 61.